Limnol. Oceanogr., 52(6), 2007, 2656–2667

The seasonal evolution of high vertical–mode internal waves in a deep reservoir

Javier Vidal
Institut de Medi Ambient, Universitat de Girona, Campus de Montilivi, 17071 Girona, Spain
Instituto del Agua, Universidad de Granada, C/Ramón y Cajal, 4, 18071 Granada, Spain

Francisco J. Rueda[1]
Instituto del Agua, Universidad de Granada, C/Ramón y Cajal, 4, 18071 Granada, Spain

Xavier Casamitjana
Institut de Medi Ambient, Universitat de Girona, Campus de Montilivi, 17071 Girona, Spain

Abstract

The causal mechanism and seasonal evolution of the internal wave field in a deep, warm, monomictic reservoir are examined through the analysis of field observations and numerical techniques. The study period extends from the onset of thermal stratification in the spring until midsummer in 2005. During this time, wind forcing was periodic, with a period of 24 h (typical of land–sea breezes), and the thermal structure in the lake was characterized by the presence of a shallow surface layer overlying a thick metalimnion, typical of small to medium sized reservoirs with deep outtakes. Basin-scale internal seiches of high vertical mode (ranging from mode V3 to V5) were observed in the metalimnion. The structure of the dominant modes of oscillation changed as stratification evolved on seasonal timescales, but in all cases, their periods were close to that of the local wind forcing (i.e., 24 h), suggesting a resonant response. Nonresonant oscillatory modes of type V1 and V2 became dominant after large frontal events, which disrupted the diurnal periodicity of the wind forcing.

Basin-scale internal waves, commonly excited by wind forcing, provide the main driving force for vertical and horizontal transport in stratified systems under the wind mixed layer (e.g., MacIntyre 1998). They constitute one of the key features in the physical environment of lakes and reservoirs related to the biogeochemical behavior of these water systems. Internal waves cause a periodic vertical displacement of the suspended biomass and thus a periodic variation in the light intensity to which algal cells are exposed (Kamykowski 1979; Gaedke and Schimmele 1991). This, in turn, influences the rate of photosynthesis (Pahl-Wostl and Imboden 1990). More recently, Serra et al. (2007) have studied the role of internal waves in determining the vertical distribution of phytoplankton. They showed that different species of phytoplankton respond differently to internal waves, depending on how individuals are distributed vertically in the water column. The distribution is determined by factors such as convectively driven turbulence, the ability of particular species to move actively in the water column or the internal waves themselves. Internal waves also contribute to the generation of bottom boundary layers (Pierson and Weyhenmeyer 1994). The induced bottom currents contribute to the mixing and resuspension of sediments in the benthic boundary layer by transporting the products of bacterial decomposition away from the sediment–water interface into the bulk water (Gloor et al. 1994). Therefore, internal waves play an important role in the ecology of aquatic systems; as a consequence, the study and description of these waves in stratified lakes has drawn a considerable amount of attention in the scientific literature (e.g., Hodges et al. 2000; Antenucci and Imberger 2003; Rueda et al. 2005, just to mention a few).

Internal waves at the basin scale have spatial characteristics and oscillation periods that, in small to medium size lakes, are controlled by the density stratification and the geometric properties of the enclosing basin. Internal wave motions can be classified according to the number of nodal points (V*i*H*j*), where *i* and *j* are the number of vertical and horizontal nodes (Fig. 1). The most commonly observed mode, the V1H1, has one vertical and one horizontal nodal point, and it is characterized by a unique recirculation cell in the containing basin. Observations of high–vertical mode internal waves are seldom reported because these modes have been traditionally deemed rare in nature (e.g., Stevens and Lawrence 1997). Second vertical modes, for example, have been reported by LaZerte (1980), Wiegan and Chamberlain (1987), and Roget et al. (1997), among others. Münnich et al. (1992) showed that the second vertical mode V2H1 is dominant in the internal wave field of Alpnacher See, a side basin of Lake Lucerne. Antenucci et al. (2000) identified vertical mode 2 and 3 basin-scale internal waves as the seasonal stratification evolved in Lake Kinneret. Also recently, Vidal et al. (2005) and Pérez-Losada et al. (2003) have presented experimental evidence of third

[1] Corresponding author (fjrueda@ugr.es).

Acknowledgments

Thanks to the Centre for Water Research (CWR, University of Western Australia) and its director, Jörg Imberger, for making both the Dynamic Reservoir Simulation Model (DYRESM) and the Estuary and Lake Computer Model (ELCOM) available for use in this project. We also are indebted to Professor John Little (Virginia Tech), who kindly agreed to revise this manuscript. This work was partially funded by the University of Granada ('Plan Propio de Investigación UGR').

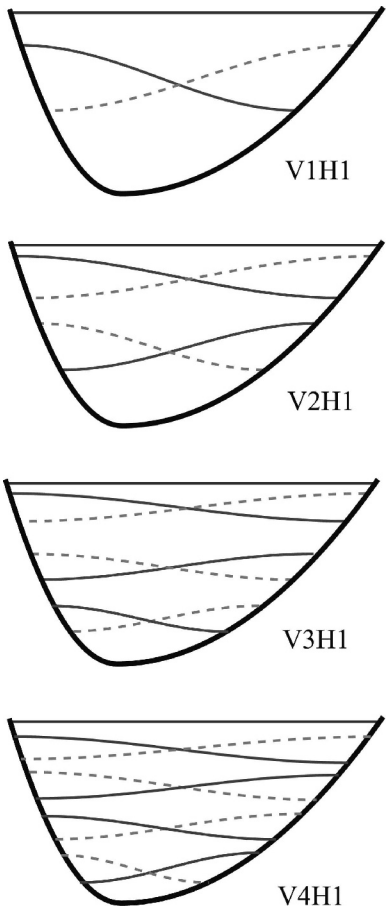

Fig. 1. The structure of internal waves of varying vertical modes.

vertical mode oscillations occurring in reservoirs forced by diurnal winds. Here, we will demonstrate, in a case study, that internal waves of high vertical modes (larger than three) can exist and even dominate the internal wave field in lakes and reservoirs. Our work will examine the causal mechanisms that explain the occurrence of these modes of oscillation. Furthermore, we will examine the seasonal evolution of the internal waves with large vertical modes.

Our study is based on the analysis of time series of water temperature collected at different depths during periods of up to several months in a small and deep reservoir with deep withdrawal structures. As shown by Casamitjana et al. (2003), in this type of system, thick metalimnetic layers develop in response to large withdrawal rates. Simple scaling arguments suggest that, in wind-forced systems with continuous stratification, waves of high vertical modes can become dominant features of the internal wave field. Koseff and Street (1985) pointed out that the number of recirculation cells in a linearly stratified lid-driven cavity flow was related to the bulk Richardson number ($\mathrm{Ri_b}$)

$$\mathrm{Ri_b} = g\frac{\Delta\rho}{\rho}\frac{D}{U_b^2} \quad (1)$$

where g is the acceleration of gravity, $\Delta\rho$ is the density difference between the top and the bottom of the cavity, ρ is a reference density, D is the depth of the cavity, and U_b is the speed of the lid or the speed of water parcels at the surface. For $\mathrm{Ri_b} >> 1$, Koseff and Street (1985) showed that at least two secondary circulation cells are present in addition to the primary cell; for $\mathrm{Ri_b} \approx 1$, a primary circulation cell will dominate the flow, whereas for values of $\mathrm{Ri_b} << 1$, the mixed layer penetrates to the lower boundary of the cavity and the circulation is similar to isothermal flow. Although Koseff and Street (1985) did not explicitly discuss wave modes in their work, one can arguably relate the number of circulation cells they observed to the structure of internal oscillations, which could have become more evident once stresses on the surface stop. For example, one circulation cell in a stratified basin will cause isopycnals to rise at the upwind end and to descend at the downwind end, exciting a V1 seiche; two cells would have caused the isotherms to stretch on the upwind end, while compressing on the downwind end, exciting V2 modes. In general, a larger number of circulation cells would have induced higher vertical modes. Surface and bottom temperatures in deep ($h_{max} > 30$ m) reservoirs in Spain during summer are typically 24°C and 10°C, respectively (Armengol et al. 1994), and the corresponding value of $\Delta\rho/\rho \approx 2.4 \times 10^{-3}$. For surface drift velocities U_b of 0 (10^{-1}) m s^{-1}, which would correspond to wind speeds of 10 m s^{-1} (e.g., *see* p. 23 in Csanady 1982), $\mathrm{Ri_b}$ is 0 (10^2). Hence, high vertical modes will likely develop in deep reservoirs in response to wind forcing.

Materials and methods

Lake Beznar—Lake Beznar is a mesotrophic reservoir located in southern Spain (Fig. 2), draining a watershed that occupies the southwestern portion of the Sierra Nevada. The watershed has a surface area of approximately 352×10^6 m^2 and changes in elevation of ~2,500 m. The average inflow, Q, that enters the reservoir from its contributing watershed is 1.79 m^3 s^{-1} (56.5×10^6 m^3 annual volume) with large oscillations on seasonal scales. Maximum inflow rates occur during winter and spring, coinciding with rain or snowmelt events. Minimum flow rates occur during late summer and early fall. The maximum volume of water held in the reservoir, V, is 54.6×10^6 m^3; hence, the nominal residence time of Lake Beznar, estimated as V/Q, is ~1 yr. When the reservoir is full, its surface area is $\sim 1.7 \times 10^6$ m^2, the elevation of the free surface is 485 m above sea level (a.s.l.), and its maximum depth is 103 m at the dam. Two outlets are located at 410 and 450 m a.s.l. The water level during the study period varied from 478 m a.s.l. to 471 m a.s.l., corresponding with maximum depths of 96 and 89 m, respectively; therefore, the shallow outtake depth was 21–28 m, and the deep outtake depth was 61–69 m.

The reservoir has an elongated shape oriented along the NW–SE direction (Fig. 2). The largest inflows occur at the northwestern end from the Izbor River. The river reach inundated by the reservoir is ~4,400 m long and rather steep (the average slope is ~0.02). The valley is wide open

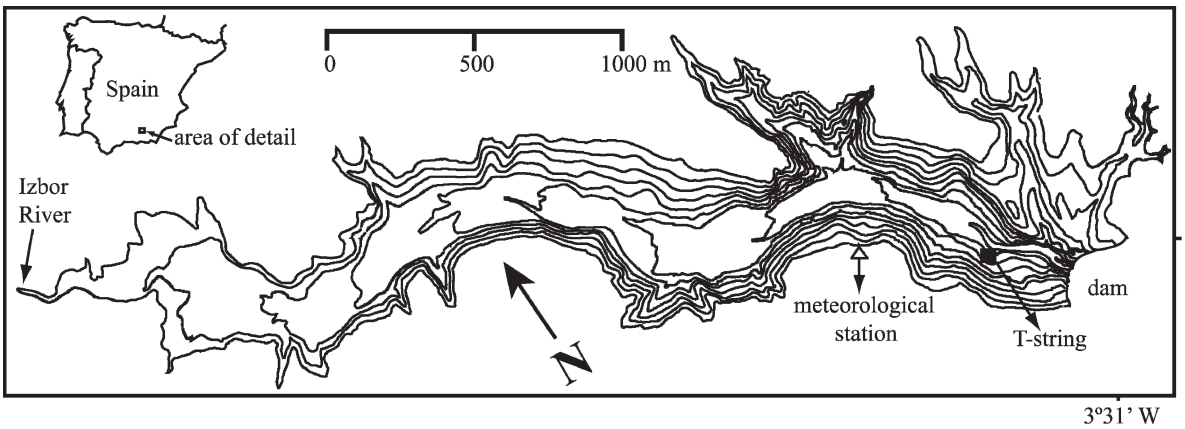

Fig. 2. Lake Beznar bathymetry showing the location of the thermistor chain and meteorological station. Isobaths are represented every 10 m.

in the tail of the reservoir, but with lateral slopes of up to 50% in the dam area.

Experimental data set—In 2005, to characterize the evolution of the internal wave field on seasonal timescales, a thermistor chain was deployed near the dam (Fig. 2) and left for 122 d, from day 95 to 217 (study period), during late spring and summer. Thermistors were deployed at the surface and at 2, 4, 6, 10, 15, 20, 25, 30, 50, and 80 m depth and were programmed to record temperature at 30-min intervals. The shallow temperature sensors (<30 m depth) were HOBO H20-001, and the remaining were Stowaway TidbiT thermistors. Hourly meteorological and daily hydrologic records were provided by the regional government of Andalucía located ~1 km north of the reservoir (36°56′52″N, 3°32′43″W). From day 155, a second meteorological station was deployed on the lake shore that collected air temperature, relative humidity, solar radiation, wind speed, and wind direction at 5-min intervals. Comparisons between both nearby and lake-shore stations showed good correlation.

Natural internal wave modes—The frequency and the spatial structure of the natural modes of the internal oscillations in Lake Beznar were analyzed with a two-dimensional eigenvalue model that was initially proposed by Münnich (1996) and recently applied by Vidal et al. (2005) to Sau Reservoir. Throughout this work, this model will be referred to as the 2D eigenmodel. It is based on the numerical solution of the generalized eigenvalue problem for the stream function ϕ in a vertical plane given by

$$\frac{\partial^2 \phi}{\partial x^2} = \frac{\omega^2}{N^2} \frac{\partial^2 \phi}{\partial z^2} \tag{2}$$

Here x and z are the along-the-thalweg and vertical coordinates, respectively; ω is the oscillation frequency of the internal wave; and N^2 is the Brunt–Väisälä or buoyancy frequency ($= -g/\rho \, d\rho/dz$, with ρ being the density of water and g the acceleration of gravity), which in general is a function of z. Lateral variations in this model are ignored. This simplifying two-dimensional assumption is deemed reasonable given the narrow and elongated shape of Lake Beznar (*see* Fig. 2). Although variations in the width of the reservoir or the sinuosity of the river valley will determine the detailed characteristics of the internal wave field, it is presumed that the overall characteristics of the mode structure and periodicity can be well represented by a two-dimensional wedge. Furthermore, the internal Rossby radius of deformation (Ro) for Lake Beznar's latitude and the stratification existing during the study period is about 900 m, and the maximum width of the lake about 400 m. Thus, the Burger number (B), defined as the ratio of Ro and the width of the reservoir is $B \approx 2 > 1$, suggesting that Earth rotation will not affect the internal motions (e.g., Cushman-Roisin 1994). The validity of the two-dimensional assumption was further supported by the simulations conducted with three-dimensional models (*see* below).

Given the large spacing between some of the thermistors and to provide the 2D model an accurate description of the thermal structure of the water column in Lake Beznar, the data were interpolated to 2 m. Linear interpolation was used above 30 m depth, whereas from 30 m to the bottom (where only three thermistors were deployed), the interpolation was exponential. This combined approach (linear–exponential interpolation) was chosen because it provided the best fit to the temperature profiles simulated (*see* Rigosi 2006) with a one-dimensional model (DYRESM, Imberger and Patterson 1981). In these simulations, water temperature below 30 m (where the withdrawal structures are located) undergoes small (<1°C) variations during the 3-month period in 2005 when the data were collected. This feature could only be captured with exponential interpolation below 30 m.

Internal waves and wind forcing—The relationship between the internal wave oscillations and the wind forcing was analyzed with a three-dimensional hydrodynamic model, which accounts for complex geometries, time variations (periodicity) of the wind acting on the free surface, and the possible influence of the Earth rotations. The model used in this work is the Estuarine and Lake Computational Model (ELCOM) initially proposed by Hodges et al. (2000) and applied to the description of the

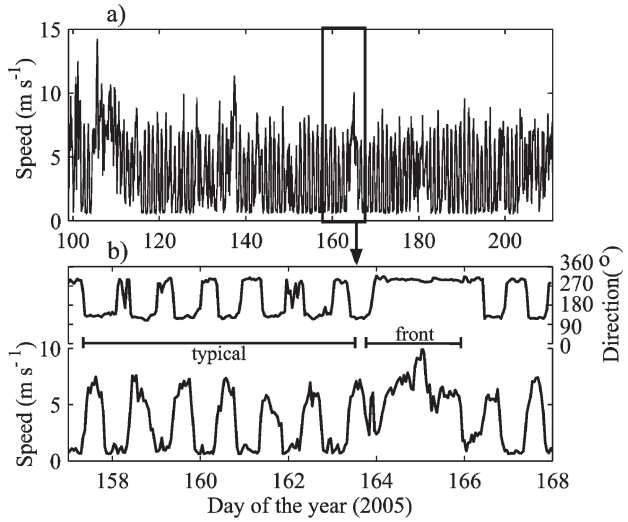

Fig. 3. (a) Wind magnitude evolution throughout the 2005 study period in Lake Beznar and (b) wind magnitude and direction for a representative period (see squared zone in panel a) in which the typical sea breeze daily pattern and the passage of a front are shown.

internal waves by Laval et al. (2003) and Gomez-Giraldo et al. (2006), among others. ELCOM solves the three-dimensional hydrostatic, Boussinesq, Reynolds-averaged Navier Stokes, and scalar transport equations. The model was initialized and forced with the use of the experimental data collected in 2005.

Results

Meteorological records—Hourly time series of local atmospheric variables were recorded at the nearby meteorological station. Air temperature records exhibited change both at diurnal and synoptic timescales. In general, temperature underwent a warming tendency during the survey up to day 200. Figure 3 shows the wind records collected during the study period. Wind forcing is regular, and most of the time, it exhibited a remarkable diurnal periodicity: maximum wind speeds occur during the afternoon (from 15:00 to 18:00 h), mostly from the southeast; lowest wind speed values occur during the night and early morning when the wind direction reverses (Fig. 3b). This pattern persists for long periods of time and is only interrupted by the passage of fronts when winds, with average hourly speeds of up to 10 m s^{-1} and predominantly from the northwest blow over the lake (Fig. 3b).

Hydrological records—Inflows and outflows control the long-term and seasonal evolution of the water level and the thermal structure in reservoirs; therefore, although indirectly, they should be considered factors explaining internal oscillations. Furthermore, inflows and, especially, outflows can be considered forcing mechanisms exciting internal waves. As shown by Imberger (1980), the onset of flow-through selective withdrawal structures (or, in general, any sudden change in the withdrawal rate) could generate shear and internal waves of a wide range of modes. If the frequency at which withdrawal rates are changed coincide with the frequency of any natural mode of oscillation in the reservoir, resonance can occur.

Inflow rates slowly decreased during the study period, from ~1.5 m^3 s^{-1} on day 95 to 1 m^3 s^{-1} on day 217. No storms occurred during this time; hence, inflow variations were smooth at diurnal timescales. Visual inspection (not shown) of the continuous water level records collected (on paper) at a gauge station located 500 m upstream of the reservoir suggest that inflows did not undergo subdiurnal variations and were very stable. River water temperatures collected during the study period ranged between 13°C on day 95 and 20°C on day 217, suggesting that the inflow formed an interflow. Withdrawal rates varied during the study period from near 0 at the start of the period to near 3 m^3 s^{-1} toward the end. Water was mainly withdrawn from the shallower outtake in the dam. Withdrawal rates are stable on subdiurnal timescales and only change in response to discrete changes in operation. Hence, at least at daily timescales, inflow and outflow forcing does not resonate with the internal waves of diurnal periodicity.

Lake thermal structure—The evolution of the thermal structure in 2005 is shown in Fig. 4. At the beginning of the study period, the reservoir is weakly stratified, with top–bottom temperature differences of up to 4°C and a thermocline at 10 m depth. The reservoir stratifies thereafter, and by the end of the study period, the metalimnion is almost 30 m thick with a temperature gradient of ~0.5°C m^{-1}. The development of thick metalimnetic layers occurs in reservoirs with deep outtakes under strong heating when the withdrawal rates are large enough to affect the stratification (Casamitjana et al. 2003). This is the case for Lake Beznar. Simple scaling arguments suggest that withdrawal rates can indeed affect stratification during the study period. From days 120 to 160, for example, water was withdrawn at an average rate of $Q_{out} \approx 1.5$ m^3 s^{-1} through the outtake located at 450 m a.s.l. The lake area at that elevation is 7×10^5 m^2. At a rate of Q_{out}, an isotherm located 1 m above the outtake (i.e., at 451 m a.s.l.) would take ~5 d to reach the level of the outtake. At that vertical velocity, an isotherm would take approximately 50 d to descend 10 m. This is, in fact, the rate at which the 14°C isotherm (located ~12 m below the free surface on day 120) descends in Fig. 4, which suggests that the seasonal evolution of the thermal stratification could also be driven by outflows. Below the 450-m outtake (the hypolimnion), the water temperature remains uniform and almost steady throughout the study period. In the metalimnion, though, water temperature undergoes oscillations at a range of scales from those typical of wind events to daily periods. In response to strong northwesterly winds associated with frontal events, the shallower isotherms descend. However, this effect mostly reflects the three-dimensional nature of wind-driven motions in enclosed basins rather than vertical mixing. On timescales on the order of individual wind events, the response of the water column to wind stress can be analyzed on the basis of the values of the Wedderburn W and Lake numbers L_N (Stevens and Imberger 1996). The

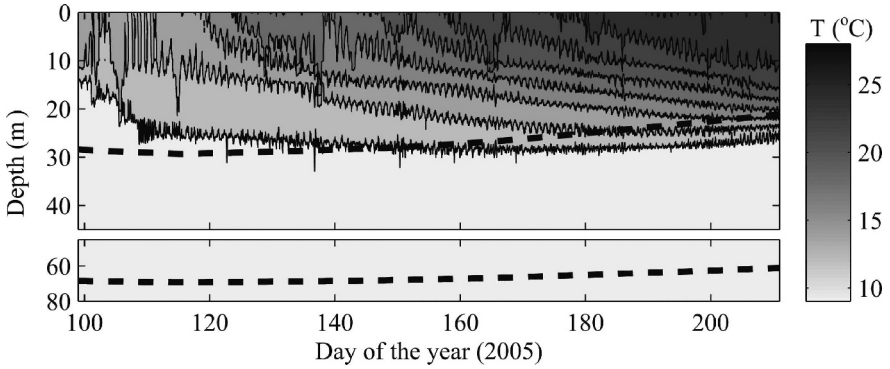

Fig. 4. Evolution of the thermal vertical structure as obtained from the thermistor chain in Lake Beznar during the study period. Figure shows isotherms every 2°C, from 12°C (deeper isotherm) to 26°C. Dashed lines indicate the depth of the outtake structures.

Wedderburn number W was calculated as (Imberger and Patterson 1990)

$$W = \frac{1}{L}\frac{g'h^2}{u_*^2} \tag{3}$$

where g' is the reduced gravity ($= g\,\Delta\rho/\rho$), h is the thickness of the surface mixed layer, and L is the basin length, here assumed to be ~4,400 m. The base of the surface layer was estimated as the depth at which the temperature is 0.2°C lower than at the surface (MacIntyre et al. 2002). The Lake number is estimated as

$$L_N = \frac{M_{bc}}{\tau A_s z_v} \tag{4}$$

where M_{bc} is the baroclinic moment about the center of the embayment volume, τ is the surface shear stress, A_s is the surface area, and z_v is the depth of the volume center. The surface shear stress was calculated from the wind speed with a simple bulk parameterization (*see* eq. 6.17 in Fischer et al. 1979) with a drag coefficient $C_D = 1.3 \times 10^{-3}$. For the calculation of M_{bc}, the location of the center of the metalimnion was estimated as follows. First the N^2 profile was estimated from interpolated daily average temperature information. Linear interpolation and smoothing was used to get profiles with 0.25-m vertical resolution. The metalimnion was defined as that part of the water column at which $N^2 > 10^{-4}$ s^{-2}. Although this limit is arbitrary, in principle, the top of the metalimnion agreed well with the depth of the mixed layer as estimated in MacIntyre et al. (2002). The depth equidistant from the top and the bottom of the metalimnion was chosen as the center of the metalimnion. Low Lake numbers ($L_N < 1$) are associated with vertical mode 1 tilting of the temperature field, whereas low Wedderburn numbers ($W \approx O[1]$ or $W < 1$) are associated with a higher vertical mode 2 response (Imberger and Patterson 1990). Our calculations for Lake Beznar suggest that during most of the study period, the response of the lake to wind forcing is characterized by $L_N >> 1$ and $W < 0.5$; only during the first 15 d of our study period, when stratification was weak, L_N was close to 1. Therefore, according to Stevens and Imberger's (1996) analysis of W and L_N, wind forcing in Lake Beznar during summer will push metalimnetic water upwind and warm surface water downwind. Isotherms in the upwind region will stretch, whereas in the downwind end of the lake, they will compress. For example, in Fig. 4, on day 165, isotherms compress and the surface layer deepens in response to strong northwesterly winds (Fig. 3).

High vertical modes under periodic conditions—The diurnal periodicity exhibited by the isotherm displacements in the upper 30 m of the water column (Fig. 4) persists throughout the study period. To analyze the internal wave field and its evolution at seasonal scales, continuous wavelet transforms were applied to time series of potential energy (PE) following Antenucci et al. (2000). The analysis was based on the PE time series and not on the isotherm displacements, given that, because of the seasonal change in temperature, no specific isotherm persisted throughout the entire period of study. Morlet wavelet transformation was used because it allows visualization of the time evolution of the frequency and intensity of the different oscillatory modes (*see* Antenucci and Imberger 2003; Naithani et al. 2003). To estimate the PE, for every time step t, a vertical temperature profile with 1-m resolution was obtained by linearly interpolating the observations in the field. The PE per unit volume was then estimated for each 1-m bin, located at z meters above the bottom and at any given time t as follows,

$$\mathrm{PE}(z, t) = \rho(z, t)gz \tag{5}$$

Here, the density ρ was derived from temperature following Chen and Millero (1977). Continuous wavelet transforms were applied to the PE time series at each individual bin, and the absolute values of the continuous wavelet signals were then integrated. The real part of the wavelet coefficients gives an insight into the energy density and the phase at a certain depth (Naithani et al. 2003). Vertically integrating the absolute value of the coefficients, we can obtain an insight of the time evolution of the energy and phase of the different modes present in the system. Given that the density variations below 30 m are small, only the density variations in the upper 30 m of the water column were used. Figure 5b shows the integrated signal of

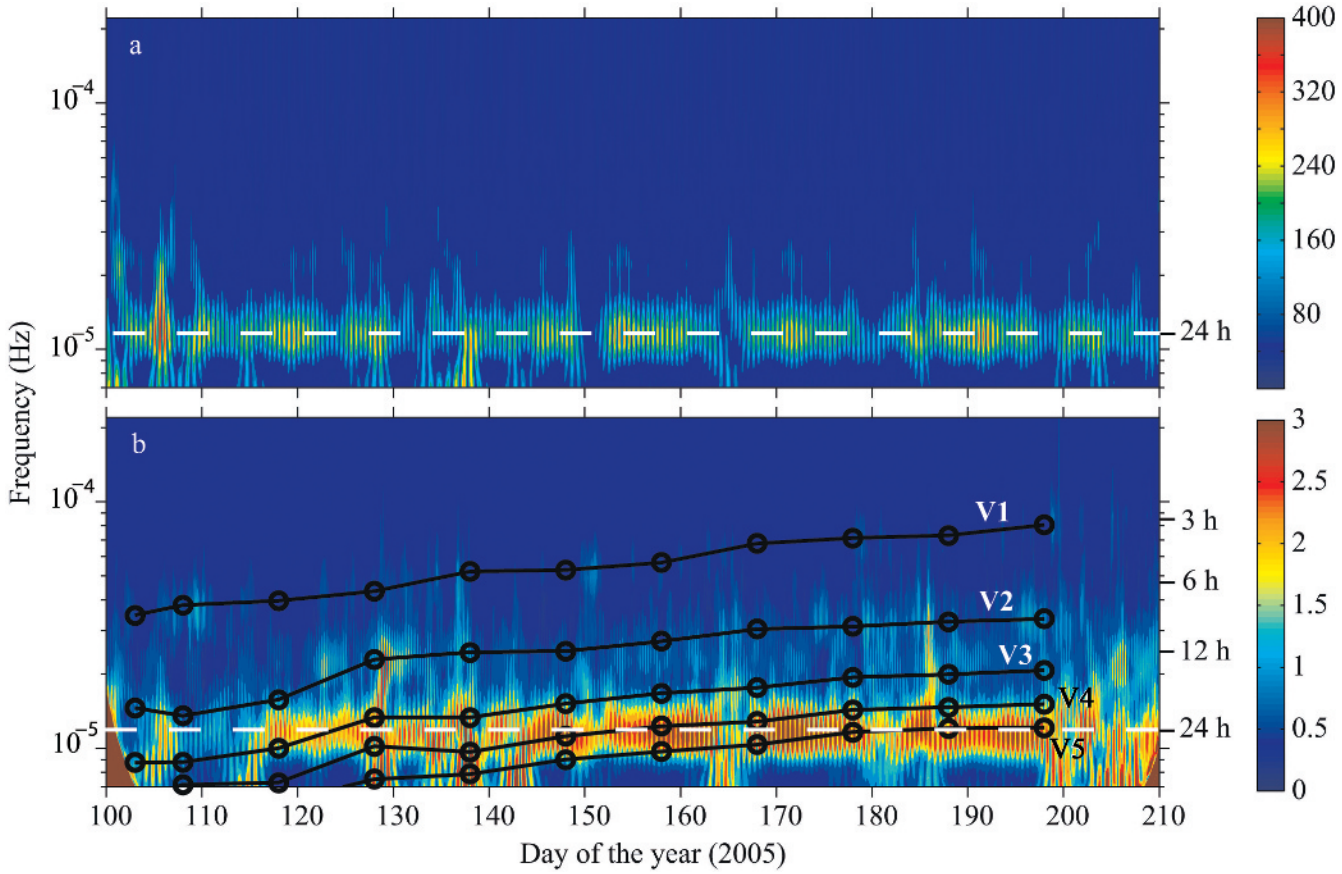

Fig. 5. (a) Real part of the continuous wavelet coefficients in absolute values of square of the wind speed and (b) real part of the integrated signal of the continuous wavelet coefficients of discretized PE along the water column (*see* text). Circles connected by black lines indicate the evolution of the frequency of the V1H1, V2H1, V3H1, V4H1, and V5H1 mode, as obtained with the 2D model.

the continuous wavelet transform of the PE in the water column.

The 24-h periodicity in the internal wave field appears to be correlated with the strong diurnal periodicity that characterizes the wind regime. Figure 5a shows the evolution of the continuous wavelet transform of the square of the wind speed obtained from the nearby meteorological station. The diurnal periodicity in wind forcing persists during most of the study period and is only disrupted by the passage of episodic fronts (*see*, e.g., day 106). Peaks at 24 h in the continuous wavelet transform of the PE signal (Fig. 5b) correspond to the peaks in the continuous wavelet transform for the wind with a small lag, which suggests a close link and a causal relationship between the 24-h internal waves and the wind forcing characterized by its diurnal periodicity (Fig. 5a). The vertical structure of the 24-h internal waves was derived by comparing the temperature records from individual thermistors. Note that temperature records, and not isotherm displacements (as is done elsewhere in the literature because it is more intuitive), are used here to visualize the vertical structure of internal waves. This approach is justified because the spacing among some of the thermistors was large, and, consequently, the result of interpolating temperature records to get isotherms was uncertain. To avoid such uncertainty in the interpretation of the vertical structure of the internal waves, it was decided to analyze temperature records, directly. In a plot showing temperature time series at any given and fixed depth, rising isotherms will cause the temperature records to decrease: cooler water from lower layers would be reaching the thermistor. By contrast, descending isotherms will cause temperature records to increase. With the use of this simple rule, one can see, for example, that between days 119 and 123, the internal wave had a V3H1 mode (*see* Fig. 6a). The modal structure of the internal wave, changes through the season, and mode V4H1 become dominant around day 160 (Fig. 6b), and even a mode V5H1 appears around day 197 (Fig. 6c). Note that the behavior of the vertical displacements shown in Fig. 6 does not correspond exactly with the theoretical structure of ideal seiches. In an ideal seiche, the phase differences between the vertical displacements of any two isotherms would be either 0° or $\pm 180^\circ$. Even though this is not strictly true in our data set, one can still identify the structure of the modes from major temperature variations. These modes correspond with the natural modes of oscillation of the stratified basin, with periods that are near 24 h. To reveal this extent, we will show that the frequency and spatial structure of the natural modes of internal oscillations determined by the 2D eigenmodel, described in the *Materials and methods* section, agree with those derived from observations.

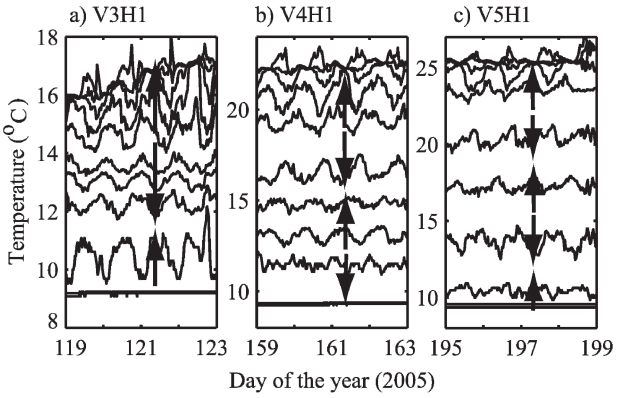

Fig. 6. Temperature observations collected at 0, 2, 4, 6, 10, 15, 20, 25, 30, 50, and 80 m depth (from top to bottom) for three different periods of time when modes (a) V3H1, (b) V4H1, and (c) V5H1 were dominant. The structure of the internal wave has been made explicit with the use of arrows, which mark the sign of the temperature change (i.e., whether temperature increases or decreases) at a given time and at different depths.

Predictions of the 2D eigenmodel were obtained every 10 d during the study period. The vertical temperature profiles used in Eq. 2 were obtained by (1) averaging in time the thermistor records corresponding to periods of 5 d and (2) interpolating the time-averaged records vertically in space, as described in the *Materials and methods* section. The estimated frequency for the natural V1H1, V2H1, V3H1, V4H1, and V5H1 modes of oscillations are shown in Table 1 and plotted as black lines in Fig. 5b. Given that Lake Beznar is relatively short (4 km) and occupies the bottom of a deep V-shaped valley with a unique branch, the wind acts nearly uniformly along the lake's thalweg, and horizontal modes >H1 should not be expected. Hence, these modes were not considered in the analysis. This assumption was later deemed valid, when inspecting the results of the three-dimensional model (see *Wind forcing and internal wave field* section). As Table 1 and Fig. 5b show, the periods of these natural modes tend to decrease as stratification evolves on seasonal timescales from early spring to late summer when top–bottom temperature differences reach their maximum. As the period of any given vertical mode gets close to 24 h, the wind forcing appears to energize it, becoming the dominant mode of oscillation over others of less spatial complexity (lower vertical mode).

Figure 7a shows the power spectral density of the temperature records collected from days 195 to 205 at 30 and 25 m. Three peaks exist in both spectra: at 24, 8.3, and 3.3 h. To determine the vertical structure of these oscillations, we calculated and studied the cross-spectra between the time series of temperature recorded at 30 m (taken as reference) and the time series of temperature recorded at other depths in which thermistors were deployed. For short periods of time, when changes in stratification are not significant, the cross-spectral analysis is an effective method to determine the vertical structure of the different modes (e.g., Münnich et al. 1992). Figure 7b shows, as an example, the cross-spectra of the temperature signals collected at 30 and 25 m. The 24-h oscillations at these two depths are coherent (as revealed by a coherence value >0.8) and have phases that differ ~180 degrees. In Fig. 7c, we have plotted the phase of the 24-h oscillations as a function of depth. The phase of the temperature oscillations with periods of 8.3 and 3.3 h are also plotted. The values of the phase shown on the abscissa represent the difference in phase relative to the temperature signal at 30 m and are given as absolute values. Note again that phases are not always exactly 0° or 180°; however, we will consider phases close to 0° as being in phase and phases close to 180° as being in opposite phase relative to the signal at 30 m. The five shifts in the phase of the 24-h signal (Fig. 7c) show that the diurnal oscillations indeed correspond to a V5 mode.

Figure 7d shows a comparison of the amplitudes of the isotherm displacements predicted by the 2D eigenmodel for mode V5H1 plotted against the amplitudes of the isotherm displacements derived directly from temperature observations. The root mean square vertical displacement (ζ_{RMS}) for any thermistor i is determined following the methodology proposed by Fricker and Nepf (2000) with details in Vidal et al. (2005). The signs (positive or negative) of the displacements at any thermistor were derived from the phase differences encountered in the cross-spectral analysis (shown in Fig. 7c) for the 24-h signal. Negative ζ_{RMS} values at any given depth in Fig. 7d indicate that the isotherm displacements at that depth and at 30 m are in phase, or their phase difference is near 0°. Positive values, in turn, indicate that the isotherm displacements are in opposite phase. The vertical structure obtained with the model agrees well with the vertical structure derived from the thermistors, especially in the shift of the vertical displacements. The largest differences between predictions and observations (in magnitude) occur mainly at the surface, which might be the result of the direct influence of the wind forcing applied to the surface layers. Note that in Fig. 7 we only show the upper 40 m of the water column for clarity in

Table 1. Periods of the main modes estimated with the 2D model along the survey from day 103 to day 198.

	Estimated period (h)										
Mode	103	108	118	128	138	148	158	168	178	188	198
V1H1	8	7.3	7	6.4	5.3	5.3	4.6	4.1	3.9	3.8	3.4
V2H1	19	20.5	17.6	12.1	11.3	11.2	10.2	9.1	8.9	8.5	8.3
V3H1	31.7	31.6	27.7	20.8	20.8	18.3	16.6	15.7	14.3	13.9	13.4
V4H1	43.7	39	38.2	27.2	28.7	24.8	22.6	21.6	19.4	18.9	18.4
V5H1	>>24	>>24	46	37	35.3	30.8	28.6	26.8	23.8	23	22.9

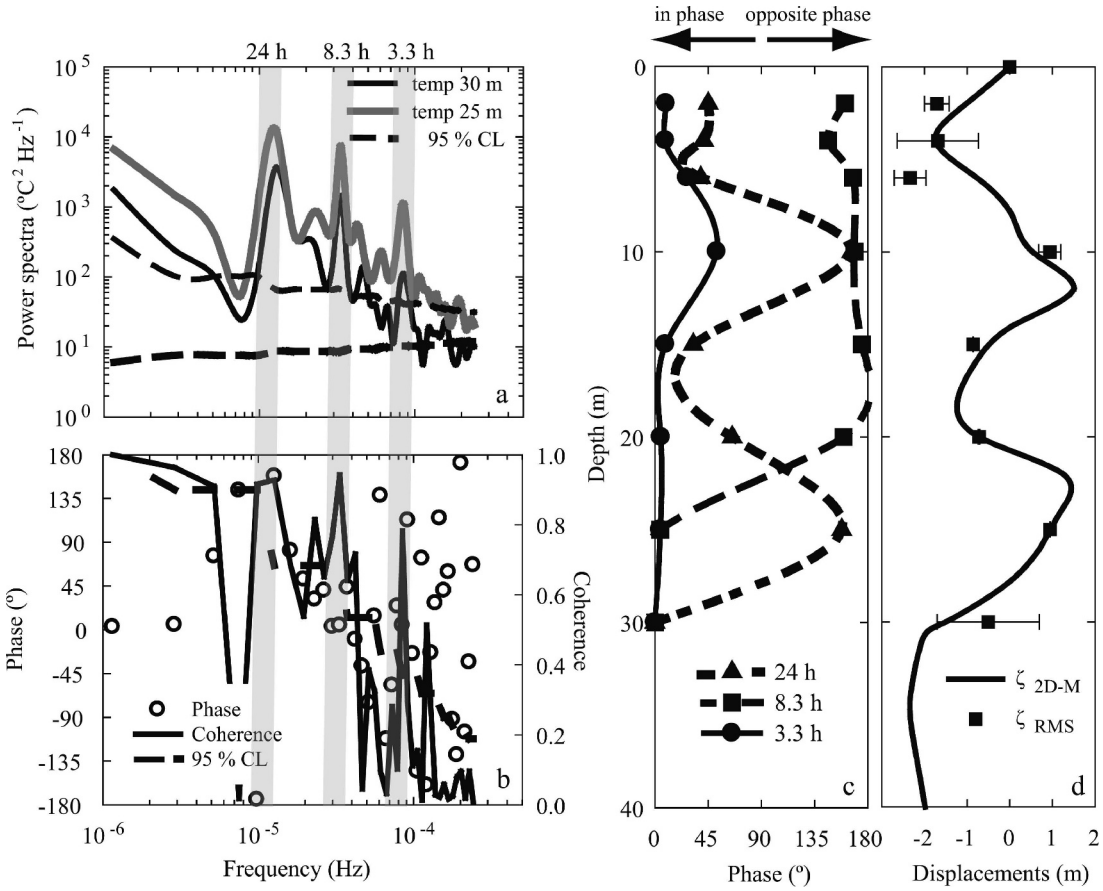

Fig. 7. (a) Power spectral density for the temperature series from days 195 to 205 (2005). (b) Coherence and phase spectra of temperature at 25 m versus temperature at 30 m. Spectra have been smoothed in the frequency domain to improve confidence; dashed line shows the 95% confidence level. (c) Phase in the water column of the main oscillatory periods (24, 8.3, and 3.3 h)—gray shadow in panels a and b. (d) Vertical displacements computed with the 2D eigenmodel ($\xi_{2D\text{-}M}$) against vertical displacements computed with the T-chain (ζ_{RMS}).

the presentation. Below 40 m, no other vertical displacements were found.

Dominant response under nonperiodic forcing—In addition to diurnal oscillations, wind events can also excite oscillatory motions at other frequencies. Peaks in the wavelet transform of the PE signal occur at periods of 24 h and also at periods that, according to the results of the 2D eigenmodel (black lines in Fig. 5b), correspond to modes V1H1 and V2H1. The spectral analysis of the temperature records collected at 25 and 30 m from days 195 to 205 (Fig. 7a) also reveals the presence of two other peaks, in addition to that corresponding to diurnal oscillation. They occur at frequencies of $\omega_1 = 3.35 \times 10^{-5}$ Hz (period $T_1 = 8.3$ h) and $\omega_2 = 8.42 \times 10^{-5}$ Hz (period $T_2 = 3.3$ h). The coherence of the signals at those two frequencies ω_1 and ω_2 is high (Fig. 7b), which suggests that they correspond to internal waves. An analysis of the phase differences in the water column reveals the vertical structure of these waves. The signal with period $T_1 = 3.3$ h corresponds to a vertical mode V1 because the temperature signals with this period oscillate in phase at all depths (*see* Fig. 7c). The signal with period $T_2 = 8.3$ h, in turn, corresponds to a mode V2: the vertical displacements in the shallower layers (from 0 to 20 m deep) oscillate in opposite phase to the deeper layers. The periods computed with the 2D eigenmodel for the stratification existing in the lake on day 198 and for modes V1H1 and V2H2 were 3.4 and 8.3 h, respectively.

Modes V2H1 and V1H1 appear throughout the study period (*see* Fig. 5). However, the energy of these modes changes both at seasonal and synoptic scales. Mode V1H1 is more energetic than mode V2H1 in late spring when thermal stratification starts to develop. Mode V2H1, in turn, becomes more energetic than mode V1H1 later in the season. This is in agreement with the Wedderburn W and Lake number L_N calculations (*see Lake thermal structure* section). Lake numbers calculated at the start of the stratified period are $L_N \approx 1$, suggesting a V1 mode response to wind events. As stratification strengthens, though, $L_N >> 1$ and $O(1)$ Wedderburn numbers suggest that mode V2H1 is probably excited by individual events. At subseasonal (synoptic scale) modes V2H1 and V1H1 become more energetic when the regular diurnal wind regime is disrupted by frontal episodic events characterized by strong northwesterly winds (*see*, e.g., days 108, 123, 129, 151, 187, or 198 in Figs. 3, 5). Given their lower damping,

compared with the higher vertical modes, V1 and V2 modes could become dominant in the system for short periods of time after the episodic wind events from the northwest. The energy locked in V1 and V2 modes, however, is small, compared with the energy locked in the 24-h oscillations under periodic wind forcing.

Wind forcing and internal wave field—The analysis shown in the previous sections suggests that (1) the reservoir has a thick metalimnetic layer with temperature gradients of up to 0.5°C m^{-1}, (2) internal waves are evidenced by the 30-min temperature records, (3) the vertical structure of the oscillations (vertical mode) changes as the stratification changes on seasonal timescales; the data reveal internal waves of up to mode V5, and (4) the dominant mode of oscillation has in all cases the same periodicity as the wind (i.e., 24 h). This picture suggests that the reservoir behaves as a forced oscillator. A well-known result in classical mechanics is that the amplitudes of the motions described by a forced harmonic oscillator depend on the energy of the forcing mechanism, the frequency of the forcing compared with the natural frequency of the oscillator, and their relative phase (*see*, e.g., Wilson 1972). These concepts are applicable to wind-forced basin-scale internal waves (Antenucci et al. 2000). When the forcing frequency coincides with that of a given natural mode of oscillation of the system, resonance occurs and that mode becomes the dominant mode of oscillation. In Lake Beznar, the dominant mode of oscillation is selected from the spectrum of possible modes by the wind forcing, which during most of the time, has a strong diurnal periodicity predominantly from the east. Our observations agree with those of Munnich (1996) and Vidal et al. (2005), in which V2H1 and V3H1 modes become dominant because of resonance with diurnal wind regimes. Other examples of resonant internal wave modes are given, for example, by Antenucci et al. (2000) and Hodges et al. (2000) in Lake Kinneret, where a V1H1 Kelvin mode (affected by the Earth's rotation) with the same 24-h period as the wind forcing becomes the dominant feature in the wave field; the seasonal evolution of the wind/internal wave field of the dominant modes was also described by Antenucci and Imberger (2003). Antenucci et al. (2000) presented, as well, an analytical model of the response of a two-layer rectangular basin undergoing internal oscillations, with the wind forcing applied impulsively. In that model, the wind amplifies the signal when a zero relative phase exists. At zero phase, the impulsive force is applied as the wave passes through zero from trough to crest and the wind energizes the internal wave. A relative phase of half the period of the internal wave, though, results in cancellation of the internal wave energy. Accordingly, we hypothesize that the strong and episodic northwesterly winds, acting out of phase with the dominant 24-h oscillations (driven by diurnal easterly sea breezes), drains energy from them and energizes V1 and V2 modes, instead.

Here, the role played by the wind field, in exciting and weakening the different modes of oscillation in Lake Beznar, is examined by means of numerical experiments in which the motion of water is simulated with a three-dimensional model (ELCOM). In these simulations, it is presumed that inflows and outflows are negligible and do not have any effect on either stratification or the internal wave field. This assumption is deemed appropriate given the short length of the simulations conducted and because the outflows did not undergo changes during the period of simulation. The model was constructed with a uniform grid of cells, $40 \times 40 \times 1$ m. It was first validated, by comparing the temperature predictions with the observations collected in the lake during a period of 10 d starting on day 188, 2005. For the validation exercise, the model was initialized with horizontal isotherms and zero velocities and forced through the free surface, with the use of momentum and heat fluxes constructed from observed meteorological variables. The initial temperature profile was constructed from temperature records collected on the first day of the validation period. This profile is the same as that provided to the 2D eigenmodel. Figure 8 compares temperature observations and simulations at different depths for the validation run. The l_1 and l_2 error norms calculated from observed and simulated temperatures, from 5 d of simulation after 2 d of warm up, with the thermistors deployed at 4, 6, 10, 15, 20, 25, and 30 m are 0.0152 and 0.0139. These values are almost one order of magnitude lower than the values reported by Hodges et al. (2000) for the simulations of internal waves in Lake Kineret.

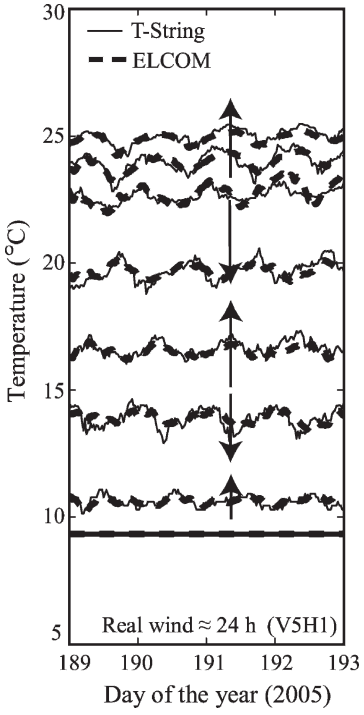

Fig. 8. Comparison of observed (thick line) and simulated temperatures (thin line) at 4, 6, 10, 15, 20, 25, 30, and 50 m depth. Simulations are conducted with the three-dimensional model ELCOM. Arrows in panel a show the number of vertical displacements.

The results of these experiments also show that the assumptions made throughout this manuscript (i.e., unimportance of rotational effects, the nature of the oscillations in the horizontal, which are presumed to be mode 1, or

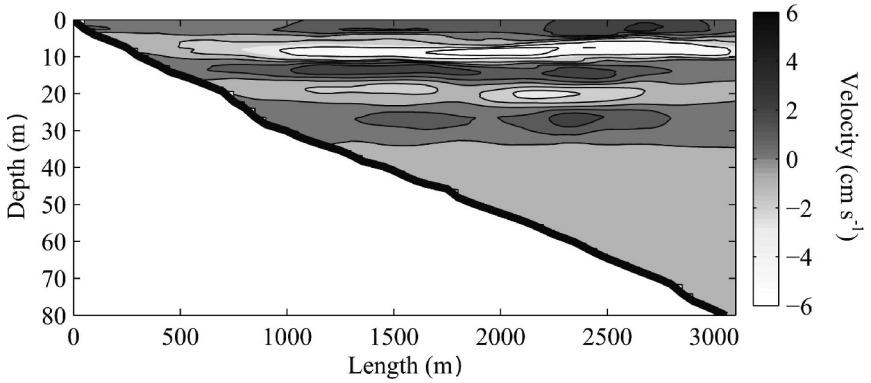

Fig. 9. Longitudinal (along the thalweg) velocity predicted by the three-dimensional model (ELCOM) on day 190.3. Positive values represent velocities toward the dam.

both) are correct. Figure 9 shows, for example, the longitudinal (along the thalweg) velocity in a vertical plane that runs parallel to the thalweg of Lake Beznar. The longitudinal velocity changes direction five times as one moves from the surface to the bottom, which is consistent with the structure of a V5H1 internal wave. It is on these planes at which the longitudinal velocity changes sign that isotherms are displaced from their equilibrium position in a horizontal plane. Note that the magnitude of the longitudinal velocity shown in Fig. 9 is subject to changes as one moves along the thalweg. Those changes are, in part, due to variations in the width of the reservoir and the sinuosity of the river valley. Similar results are obtained by setting the Coriolis parameter to zero, supporting our decision to neglect the rotational effects.

Once validated, the model was used to conduct experiments in which the lake is forced by a synthetic wind time series of sinusoidal form. The heat fluxes are neglected in this series of simulations. The amplitude of the wind forcing was set to 6 m s^{-1}, the average maximum speed observed over the reservoir. Its frequency was varied and selected from the range of frequencies predicted by the eigenmodel for the natural modes of oscillation on day 188 (*see* Table 1). The periods of the wind forcing tested are T_1 = 3.8, T_2 = 8.5, T_3 = 13.9, and T_4 = 18.9 h, corresponding to modes V1H1, V2H1, V3H1, and V4H1, respectively. The estimated period of the V5H1 mode is 23 h, and this mode was selected as the dominant mode of oscillation with winds of diurnal periodicity (Fig. 8). The response of the reservoir to different forcing periodicities is shown in Fig. 10a–d. Note that isotherm displacements are used here to display the results, rather than the temperature fields (as was done to display the observations). Isotherm plots are preferred here because (1) they provide a very intuitive manner of visualizing internal waves and (2) the interpolation exercise to get the isotherm location is done from temperature values given at 1-m intervals; hence, the error in the location of the isotherms is lower than the magnitude of the isotherm displacement. The dominant oscillation mode is V1H1 when forced at a wind period of 3.8 h (Fig. 10a), V2H1 when forced at 8.5 h (Fig. 10b), V3H1 in response to 13.9-h forcing (Fig. 10c), and finally, V4H1 in response to the 18.9-h forcing (Fig. 10d). This series of experiments suggest that the dominance of higher vertical modes (up to mode V5) in the internal wave field in Lake Beznar is the result of resonance.

Several factors, like stratification, morphology, or forcing agent, control the internal wave field in aquatic systems. In general, lower modes of oscillations are favored, given that high vertical modes are subject to larger levels of damping (e.g., Münnich et al. 1992). In Lake Beznar and, in general, in deep reservoirs with large heat fluxes and deep submerged withdrawal structures draining large volumes of water, the thermal structure is characterized by thick metalimnetic layers with nearly continuous stratification (linear). In these types of systems (continu-

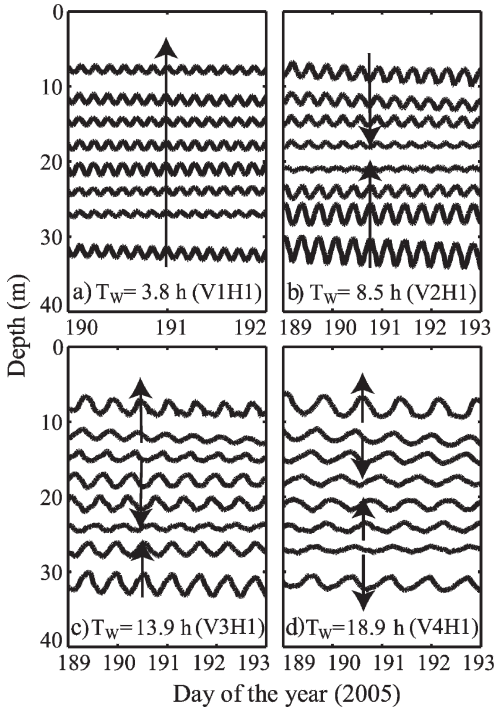

Fig. 10. Simulated vertical displacement of selected isotherms in response to synthetic and periodic wind forcing, with periods (a) T_1 = 3.8 h, (b) T_2 = 8.5 h, (c) T_3 = 13.9 h, and (d) T_4 = 18.9 h. Arrows in panels c, d show the number of vertical displacements.

ously stratified), the spectrum of internal oscillations is dense, and, a priori, any forcing frequency can lead to resonance in the seiching phenomena. In Lake Beznar, resonance with strong diurnal wind periodicity resulted in an internal wave field dominated by high vertical modes from V3H1 to V5H1. The dominant mode of oscillations changed as the stratification evolved at seasonal timescales: in May, the dominant mode had a V3 structure, whereas later in the season (mid-July), the dominant mode was V5. Lower modes of oscillations (V1H1 and V2H1) were, in turn, excited when the diurnal periodicity of the wind was disrupted. Nevertheless, such modes were much less energetic than those that were resonant under periodic wind conditions. These results suggest, that, not just V2 modes can be excited under $O(1)$ values of W and $L_N >> 1$, as stated by Imberger and Patterson (1990). If resonant with wind forcing, higher vertical modes can also be excited in systems with continuous stratification. The presence of high vertical modes have seldom been described in the literature and modes higher than V3H1, to our knowledge, have never been observed, probably because of the high levels of damping in most lakes. In this study, we show that the presence of high vertical modes is not such a rare feature in medium-sized reservoirs with thick metalimnia in which the wind periodicity plays a fundamental role in the excitation of the dominant modes. The occurrence of internal waves of high vertical modes could have implications for the physical or biogeochemical behavior of lakes and reservoirs. Driven by internal waves of high vertical modes, the metaliminon behaves effectively as if it comprised several layers. In each of those layers, water would be moving back and forth from the inflow region to the dam. Through this back-and-forth motion, waves could be creating preferential routes for lateral spreading of dissolved or suspended matter from nearshore to pelagic regions. Fischer and Smith (1983), for example, suggested that internal waves interacting with inflow gravity currents could result in the formation of intrusion structures carrying river water at levels above the theoretical depth of neutral buoyancy. Hence, the pathways of river nutrients in the reservoir could, in fact, be strongly determined by the internal waves. These waves would also determine the distribution of suspended matter and phytoplankton, with passive or active vertical motions. Hence, the analysis of the structure of the internal wave motions seems to be the first step toward understanding the space–time distribution of suspended and dissolved substances in lakes, which, in turn, determines the biogeochemical behavior of these systems.

References

Antenucci, J. P., and J. Imberger. 2003. The seasonal evolution of wind/internal wave resonance in Lake Kinneret. Limnol. Oceanogr. **48:** 2055–2061.

———, ———, and A. Saggio. 2000. Seasonal evolution of the basin scale internal wave field in a large stratified lake. Limnol. Oceanogr. **45:** 1621–1638.

Armengol, J., J. Toja, and A. Vidal. 1994. Seasonal rhythm and secular changes in Spanish reservoirs, p. 237–253. *In* R. Margalef [ed.], Limnology now: A paradigm of planetary problems. Elsevier.

Casamitjana, X., T. Serra, C. Baserba, and J. Pérez. 2003. Effects of the water withdrawal in the stratification patterns of a reservoir. Hydrobiologia **504:** 21–28.

Chen, C. T., and F. J. Millero. 1977. The use and misuse of pure water PVT properties for lake waters. Nature **266:** 707–708.

Csanady, G. T. 1982. Circulation in the coastal ocean. Reidel.

Cushman-Roisin, B. 1994. Introduction to geophysical fluid dynamics. Prentice Hall.

Fischer, H. B., E. J. List, R. C. Y. Koh, J. Imberger, and N. H. Brooks. 1979. Mixing in inland and coastal waters. Academic.

———, and R. D. Smith. 1983. Observations of transports to surface waters from a plunging inflow to Lake Mead. Limnol. Oceanogr. **28:** 258–272.

Fricker, P. D., and H. M. Nepf. 2000. Bathymetry, stratification, and internal seiche structure. J. Geophys. Res. **105:** 14,237–14,251.

Gaedke, U., and M. Schimmele. 1991. Internal seiches in Lake Constance: Influence on plankton abundance at a fixed sampling site. J. Plankton Res. **13:** 743–754.

Gloor, M., A. Wüest, and M. Munnich. 1994. Benthic boundary mixing and resuspension induced by internal seiches. Hydrobiologia **284:** 59–68.

Gómez-Giraldo, A., J. Imberger, and J. P. Antenucci. 2006. Spatial structure of the dominant basin-scale internal waves in Lake Kinneret. Limnol. Oceanogr. **51:** 229–246.

Hodges, B. R., J. Imberger, A. Saggio, and K. B. Winters. 2000. Modeling basin-scale internal waves in a stratified lake. Limnol. Oceanogr. **45:** 1603–1620.

Imberger, J. 1980. Selective withdrawal: A review, p. 381–400. *In* T. Carstens and T. McClimans [eds.], Second International Symposium on Stratified Flows. Vol. 2. The Norwegian Institute of Technology. Trondheim, Norway.

———, and J. C. Patterson. 1981. A dynamic reservoir simulation model—DYRESM: 5, p. 310–367. *In* H. B. Fischer [ed.], Transport models for inland and coastal waters. Academic.

———, and ———. 1990. Physical limnology, p. 303–475. *In* T. Wu [ed.], Advances in applied mechanics. V. 27. Academic.

Kamykowski, D. 1979. The growth response of a model *Gymnodinium splendens* in stationary and wavy water columns. Mar. Biol. **50:** 289–303.

Koseff, J. R., and R. L. Street. 1985. Circulation structure in a stratified lid-driven cavity flow. J. Hydrol. Div. ASCE **111:** 334–354.

Laval, B., J. Imberger, B. Hodges, and R. Stoker. 2003. Modeling circulation in lakes: Spatial and temporal variations. Limnol. Oceanogr. **48:** 983–994.

LaZerte, B. D. 1980. The dominating higher order vertical modes of the internal seiche in a small lake. Limnol. Oceanogr. **25:** 846–854.

MacIntyre, S. 1998. Turbulent mixing and resource supply to phytoplankton, p. 539–567. *In* J. Imberger [ed.], Physical processes in lakes and oceans. Coastal and Estuarine Studies. American Geophysical Union.

———, J. R. Romero, and G. W. Kling. 2002. Spatial-temporal variability in mixed layer deepening and lateral advection in an embayment of Lake Victoria, East Africa. Limnol. Oceanogr. **47:** 656–671.

Münnich, M. 1996. Influence of bottom topography on internal seiches in stratified media. Dyn. Atmos. Oceans **23:** 257–266.

Münnich, M. A., A. Wüest, and D. M. Imboden. 1992. Observations of the second vertical mode of the internal seiche in an alpine lake. Limnol. Oceanogr. **37:** 1705–1719.

NAITHANI, J., E. DELEERSNIJDER, AND P. D. PLISNIER. 2003. Analysis of wind-induced thermocline oscillations of Lake Tanganyika. Environ. Fluid Mech. **3:** 23–39.

PAHL-WOSTL, C., AND D. IMBODEN. 1990. Dyphora—a dynamic model for the rate of photosynthesis of algae. J. Plankton Res. **12:** 1207–1221.

PEREZ-LOSADA, J., E. ROGET, AND X. CASAMITJANA. 2003. Evidence of high vertical wave-number behaviour in a continuously stratified reservoir. J. Hydraulic Eng. **129:** 734–737.

PIERSON, D. C., AND G. A. WEYHENMEYER. 1994. High resolution measurements of sediment resuspension above an accumulation bottom in a stratified lake. Hydrobiologia **284:** 43–57.

RIGOSI, A. 2006. A physical–ecological model of Lake Beznar ecosystem. Propagation of uncertainty from physical to population dynamic predictions. Master's thesis, Univ. of Granada, Granada, Spain.

ROGET, E., G. SALVADÉ, AND F. ZAMBONI. 1997. Internal seiche climatology in a small lake where transversal and second vertical modes are usually observed. Limnol. Oceanogr. **42:** 663–673.

RUEDA, F. J., S. G. SCHLADOW, S. G. MONISMITH, AND M. T. STACEY. 2005. On the effects of topography on wind and the generation of currents in a large multi-basin lake. Hydrobiologica **532:** 139–151.

SERRA, T., J. VIDAL, J. COLOMER, X. CASAMITJANA, AND M. SOLER. 2007. The role of surface vertical mixing in phytoplankton distribution in a stratified reservoir. Limnol. Oceanogr. **52:** 620–634.

STEVENS, C., AND J. IMBERGER. 1996. The initial response of a stratified lake to a surface shear stress. J. Fluid Mech. **312:** 39–66.

STEVENS, C. L., AND G. A. LAWRENCE. 1997. Estimation of wind-forced internal seiche amplitudes in lakes and reservoirs, with data from British Columbia, Canada. Aquat. Sci. **58:** 1–19.

VIDAL, J., X. CASAMITJANA, J. COLOMER, AND T. SERRA. 2005. The internal wave field in Sau reservoir: Observation and modeling of a third vertical mode. Limnol. Oceanogr. **50:** 1326–1333.

WIEGAND, R. C., AND V. CHAMBERLAIN. 1987. Internal waves of the second vertical mode in a stratified lake. Limnol. Oceanogr. **32:** 29–42.

WILSON, B. W. 1972. Seiches, p. 1–92. *In* V. T. Chow [ed.], Advances in hydrosciences. Academic.

Received: 14 November 2006
Accepted: 5 July 2007
Amended: 5 July 2007